Targeting a *Pneumocystis carinii* Group I Intron with Methylphosphonate Oligonucleotides: Backbone Charge Is Not Required for Binding or Reactivity†

Matthew D. Disney, Stephen M. Testa,‡ and Douglas H. Turner*

Department of Chemistry, University of Rochester, Rochester, New York 14627-0216

Received December 23, 1999; Revised Manuscript Received March 31, 2000

ABSTRACT: *Pneumocystis carinii* is a mammalian pathogen that contains a self-splicing group I intron in its large subunit rRNA precursor. We report the binding of methylphosphonate/DNA chimeras and neutral methylphosphonate oligonucleotides to a ribozyme that is a truncated form of the intron. At 15 mM Mg^{2+}, the nuclease-resistant all-methylphosphonate hexamer, d(AmTmGmAmCm)rU, with a sequence that mimics the 3′ end of the precursor's 5′ exon, binds with a dissociation constant of 272 nM. The hexamer's dissociation constant for binding by base-pairing alone to the ribozyme's binding site sequence is 8.3 mM. Thus there is a 30 000-fold binding enhancement by tertiary interactions (BETI), which is close to the 60 000-fold enhancement previously observed with the all-ribo hexamer, r(AUGACU). Evidently, backbone charge and 2′ hydroxyl groups are not required for BETI. At 3−15 mM Mg^{2+}, the all-methylphosphonate and DNA oligonucleotides trans-splice to a truncated form of the rRNA precursor, but do not compete with cis-splicing when pG is present. These results suggest that uncharged or partially charged backbones may be used to design therapeutics to target RNAs through binding enhancement by tertiary interactions and suicide inhibition strategies.

Antisense nucleic acids have drawn considerable attention in recent years due to the wealth of known nucleic acid sequences**.** Antisense nucleic acids act by base-pairing to their target, thereby disrupting the normal function of an RNA (*1*). This target recognition occurs only by base-pairing and has several potential complications because long sequences, typically 15−20 nucleotides, are employed. Such long sequences can have nonspecific interactions with other sites (*2*), are expensive to synthesize (*3*), and exhibit decreased cellular uptake when compared to smaller oligonucleotides (*4, 5*). Incorporating structural and/or mechanistic information into this "rational design" can allow development of shorter, more effective antisense agents.

The wealth of information known about RNA self-splicing by group I introns (*6*−*8*) provides an opportunity to expand rational design principles for targeting RNA. For example, details about group I intron reaction mechanisms, folding thermodynamics, and substrate recognition can be used (*9*−*19*). In particular, recognition of the 5′ splice site occurs in two steps: first, the RNA substrate base-pairs with the internal guide sequence (IGS[1]) in the intron to form the P1 helix (Figure 1); second, the helix formed upon base-pairing docks into the catalytic site and forms tertiary contacts (*10*, *14*). Docking is followed by two separate transesterification reactions. This recognition by tertiary contacts and exploitation of chemical reactivity can be used for targeting group I introns.

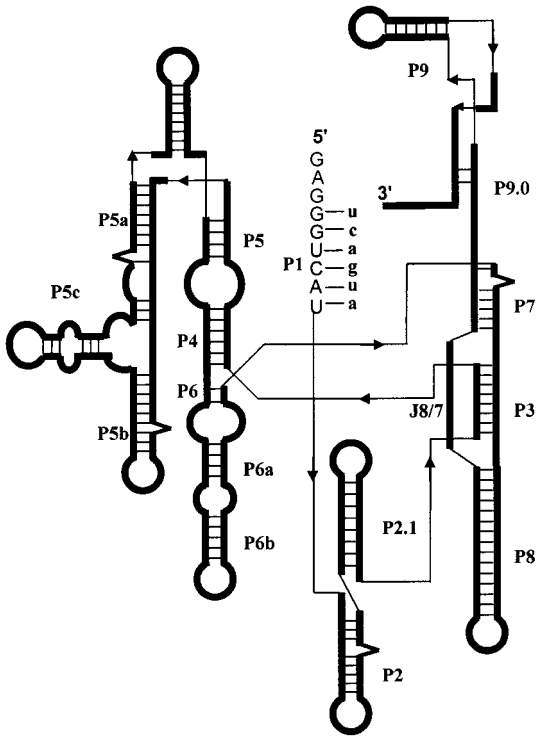

FIGURE 1: Schematic of the group I ribozyme derived from the large subunit rRNA from mouse *P. carinii* (*24*). The internal guide sequence (IGS) is in upper-case letters and the 5′ exon mimic is in lower-case letters.

† This work was supported by NIH Grant AI45398.

* To whom correspondence should be addressed. Phone: (716) 275-3207. Fax: (716) 473-6889. E-mail: Turner@chem.rochester.edu.

‡ Current address: Department of Chemistry, University of Kentucky, Lexington, KY 40506.

[1] Abbreviations: AIDS, acquired immune deficiency syndrome; ATP, adenosine triphosphate; BSA, bovine serum albumin; DTT, dithiothreitol; EDTA, ethylenediaminetetraacetic acid; Hepes, *N*-[2-hydroxyethyl]piperazine-*N*′-[2-ethanesulfonic acid]; HPLC, high-performance liquid chromatography; IGS, internal guide sequence; pG, guanosine 5′ monophosphate; NTPs, ribonucleotide triphosphates; rRNA, ribosomal ribonucleic acid; Tris, tris[hydroxymethyl]aminomethane.

10.1021/bi992937m CCC: $19.00
Published on Web 05/17/2000

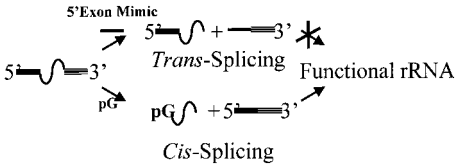

FIGURE 2: Cis- and trans-splicing reactions. In the presence of pG, the cis-splicing reaction yields normally spliced RNA where the 5′ exon and the 3′ exon become ligated to form mature rRNA. Reactions performed in the presence of some 5′ exon mimics yield trans-spliced products. These dead-end products do not allow formation of mature rRNA.

Targeting group I introns is pharmacologically relevant because several human pathogens contain self-splicing group I introns, whereas humans do not (*20, 21*). If the self-splicing activity of a group I intron is inhibited, the organism cannot form mature rRNA and presumably cannot propagate (*22*). One fungal pathogen that contains group I introns is *Pneumocystis carinii*, which infects immunocompromised hosts such as cancer and AIDS patients (*23, 24*). Current therapeutics used to treat pneumonitis, the illness caused by *P. carinii*, can induce side effects so severe that many patients must discontinue treatment (*25, 26*). In addition, fungal pathogens are evolving resistance to known treatments (*27*). Thus there is a need for new approaches to targeting *P. carinii* and other fungal pathogens.

Previous research has shown that oligonucleotide hexamers with a sequence that mimics the 3′ end of the precursor's 5′ exon will bind to the *P. carinii* intron via tertiary interactions and inhibit the splicing of a truncated form of the *P. carinii* large subunit rRNA precursor (*24, 28, 29*). Specifically, the contributions that tertiary interactions make to intron binding were determined for DNA, phosphorothioate, and phosphoramidate oligonucleotides (*24, 28*). In some cases, the oligonucleotides bind to the intron 100 000-fold more tightly than to a hexanucleotide whose sequence mimics the binding site (*28*). Furthermore, the phosphoramidate hexanucleotide can inhibit normal splicing by reacting in a manner that mimics the second step of self-splicing (*29*) (Figure 2). At 2−3 mM Mg^{2+}, the result is that a trans-spliced product is formed because the exogenous phosphoramidate outcompetes the endogenous 5′ exon for ligation to the 3′ exon. This reaction causes the formation of dead-end products, i.e., products that do not allow formation of biologically active structures. Thus, group I introns can be specifically targeted and their function inhibited by a hexanucleotide.

While much is known about interactions of oligonucleotides with group I introns, little is known about the interactions of oligonucleotides with fungi. For example, cellular uptake, compartmentalization, and degradation may depend on the oligonucleotide's chemical structure. Before testing cellular responses to various oligonucleotides, it is important to know what modifications allow exploitation of binding enhancement by tertiary interactions (BETI) and exploitation of chemical reactivity. Here, we report the effects on binding and reactivity of a hexanucleotide with the *P. carinii* group I intron (Figure 1) when backbone charge is reduced by substituting negatively charged phosphodiester linkages with uncharged methylphosphonate linkages (Figure 3). Because methylphosphonates are stereotopic, both the positional and stereochemical effects of substitutions can be determined. Furthermore, eliminating charges may increase uptake of these agents by cells.

Our results show that the stereochemistry of a methylphosphonate substitution does not have a significant effect on binding, and in all cases BETI is observed. Also, the uncharged methylphosphonate hexanucleotide, whose sequence mimics that of the 3′ end of the 5′ exon, can react with a truncated large subunit ribosomal RNA precursor to yield trans-spliced products. When compared to the same sequence with regular phosphodiester bonds, i.e., the DNA analogue, the methylphosphonates exhibit similar reactivity.

Coupling the advantages of smaller sequences with eliminating the backbone charge by using methylphosphonate nucleotides offers several potential advantages. Methylphosphonates are nuclease resistant and are taken up by cells (*30*). Moreover, smaller molecules should be more effective for targeting RNA splicing because they have a better chance to enter a cell's nucleus (*31*), where splicing occurs.

MATERIALS AND METHODS

Buffers. HXMg buffer is 50 mM Hepes (25 mM NaHepes), 135 mM KCl, and X mM $MgCl_2$ (for Hepes buffer, the ΔpK_a/°C is −0.014 (*32*)). The H15Mg buffer at pH 7.5 was used in all binding assays and optical melting studies; HXMg buffer at pH 6.5 was used in all precursor reactivity experiments to reduce hydrolysis at intron−exon junctions. TBE buffer is 100 mM Tris, 90 mM boric acid, and 1 mM EDTA at pH 8.4. Stop buffer contains 8 M urea, 8 mM Na_2-EDTA, and 0.1X TBE buffer. The 4X RNA transcription buffer contains 40 mM Tris·HCl, 5 mM spermidine, 5 mM

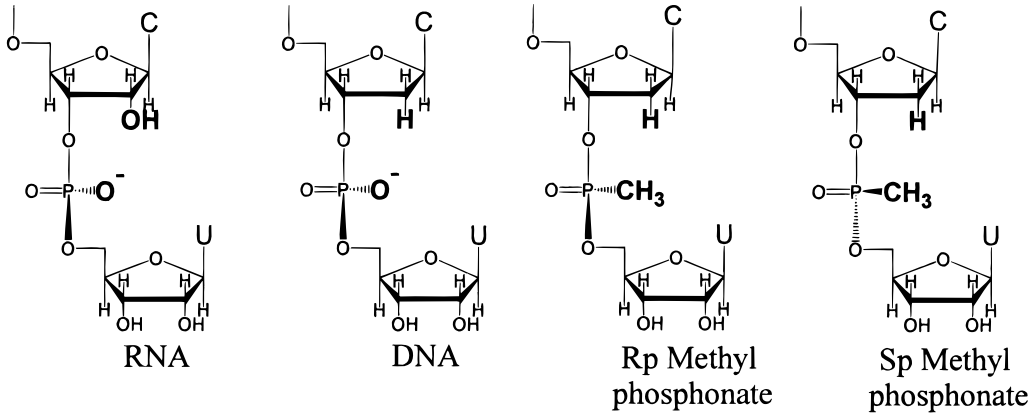

FIGURE 3: The 3′ ends of the oligonucleotides used in this study, labeled according to their backbones.

DTT, 40 mM $MgCl_2$, and 1 mM of each NTP at pH 7.5 (*24*). The 2 M TEAA buffer was made by adding reagent grade triethylamine to a solution containing 2 M glacial acetic acid until the pH reached 7.5.

Instruments. All HPLC chromatographs were obtained on a Hewlett-Packard series 1100 HPLC with an attached UV−vis detector sampling at 254 nm. Oligonucleotides were synthesized with β-cyanoethyl phosphoramidites (Glen Research, Baltimore, MD) on an Applied Biosystems 392 RNA/DNA synthesizer. Optical melting experiments were performed on a Gilford 250 UV−Vis spectrophotometer equipped with a 2527 temperature programmer. All radioactive gels were placed on chromatography paper and dried in a gel drier, and the radioactivity was quantified on a Molecular Dynamics phosphorimager with ImageQuaNT v. 4.1 software.

Oligonucleotide Synthesis and Purification. Standard phosphoramidite chemistry was used to synthesize RNA oligonucleotides from monomers with 2′ hydroxyls protected as the *tert*-butyl-dimethylsilyl ether (*33*−*36*). After completion of the RNA synthesis, the support was air-dried, and the oligonucleotide was removed from the support and deprotected by treatment with ethanolic ammonia (3:1 ammonia/ethanol) at 55 °C overnight (*35, 36*). The 2′-silyl group was removed by treatment with freshly made 1.0 M triethylammonium fluoride (50 equiv) in pyridine at 55 °C for 48 h. The crude samples were dried, desalted with a Sep-Pak C-18 cartridge (Waters), and purified on an Si500F thin-layer chromatography plate (Baker) developed with 1-propanol/ammonia/water (55:35:10 by volume). The plate was visualized with ultraviolet light, and the most intense band was eluted with sterile water.

DNA oligonucleotides were synthesized trityl-on based on the literature and using the manufacturer's standard protocol. DNA was deblocked in 0.5 mL of ammonium hydroxide for 12 h at 55 °C. The deblocked trityl-on DNA oligonucleotides were filtered from their support and then separated from failed sequences via a Poly Pak cartridge (Glen Research) using the standard trityl-on protocol.

Oligonucleotide methylphosphonates (*37*−*39*) were synthesized in the same way as DNA except that methylphosphonate monomers required a 6 min coupling time. Oligonucleotide methylphosphonates and DNA/methylphosphonate chimeras were deblocked in 0.5 mL of 45:45:10 acetonitrile/ethanol/ammonium hydroxide for 30 min, and then 0.5 mL of ethylenediamine was added for 6 h, all at room temperature (*40*). This deblocking method was used to eliminate transamination products that occur at cytosines when the oligonucleotides are deblocked with ethylenediamine alone (*40*). Methylphosphonate oligonucleotides were purified via HPLC on a Supelco ABZ +Plus column, with a running buffer of 100 mM TEAA, a flow rate of 1.5 mL/min, and a linear gradient of 0 to 50% acetonitrile over 40 min. Because of the 32 stereoisomers in the all-methylphosphonate hexamer, several HPLC peaks were observed. HPLC injection of the trityl-on oligonucleotide, however, gave only one peak. The trityl-on oligonucleotide was collected and then detritylated in 80% aqueous acetic acid. The detritylated oligonucleotide was then desalted with a Poly Pak cartridge. The identity of two methylphosphonate oligonucleotides was confirmed by electrospray mass spectrometry on a Hewlett-Packard series 1100 LC/MS Chemstation: d(AmTmG-mAmCm)rU (calculated 1784, experimental 1783) and d(AmTmGmAC)rU (calculated 1786, experimental 1788).

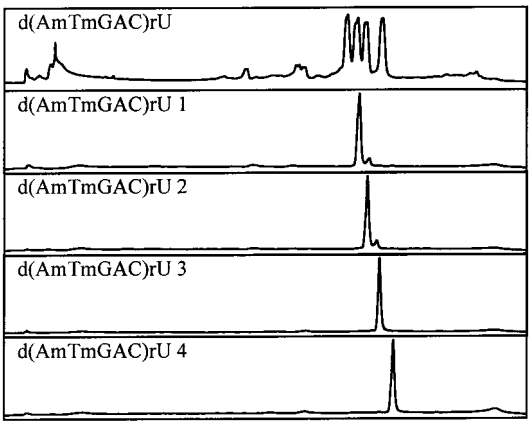

FIGURE 4: HPLC separation of methylphosphonate stereoisomers for the sequence d(AmTmGAC)rU. Stereoisomers were separated on a Supelco ABZ +Plus column; the running buffer was 100 mM TEAA, with a flow rate of 1.0 mL/min, and a linear gradient of 0 to 50% acetonitrile over 80 min. The top trace represents a typical chromatograph for a crude isomeric mixture. As expected, the synthesis contains four stereoisomers, an *R,R*, an *S,S*, an *R,S*, and an *S,R*. All four stereoisomers were isolated, concentrated, and reinjected (bottom four traces). The two peaks seen in the second and third chromatographs are due to contamination of one stereoisomer with the other. All stereoisomers were at least 90% pure.

The purity of oligonucleotides was evaluated by HPLC using a Supelco ABZ +Plus or a Hamilton PRP-1 column. The HPLC buffer was 100 mM TEAA, the flow rate was 1.5 mL/min, and a linear gradient of 0 to 50% acetonitrile over 40 min was used. The RNA, DNA, and all-methylphosphonate oligonucleotides were at least 95% pure.

Methylphosphonate/DNA chimera stereoisomers were separated by HPLC on a Supelco ABZ +Plus column. The running buffer was 100 mM TEAA, with a flow rate of 1.0 mL/min, and a linear gradient of 0 to 50% acetonitrile over 80 min was used (Figure 4). Fractions containing each individual stereoisomer were collected and concentrated. Residual TEAA was removed via repetitive coevaporations with water and/or ethanol until a white or off-white solid was obtained. All stereoisomers were re-injected after collection and concentration, and were at least 90% pure. All oligonucleotides were stored in sterile water at −20 °C.

Precursor and Ribozyme Synthesis and Radiolabeling. The P-h precursor and P-8/4x ribozyme were transcribed, and the precursor was internally (*24*) and 3′ end-labeled (*29*) as described previously. The internally labeled precursor was synthesized via runoff transcription with 5 μL of 200 ng/μL linearized plasmid added to 5 μL of 4X transcription buffer, 5 μL of α^{32}P-labeled ATP (New England Nuclear, 10 μCi/μL), and 100 units of T7 RNA polymerase, to a total volume of 20 μL. The reaction was incubated for 75 min at 37 °C and run through a Chroma spin 10 column (Clontech) to remove the unincorporated α^{32} ATP. Reaction products were purified on a 5% polyacrylamide, 8 M urea gel and isolated via the crush and soak method. Isolated products were ethanol-precipitated twice, dissolved in 200 μL of sterile water, and stored at −20 °C.

The precursor was 3′ end-labeled in a reaction mixture containing 50 mM Hepes (pH 8.3), 10 mM $MgCl_2$, 10 μg/μL BSA, 7.0 μM precursor, 7.6 μL of pCp (New England

Nuclear, 10 μCi/μL), 2 mM ATP, and 35.2 units of T4 RNA ligase (Gibco) to a total volume of 27 μL (*29*, *41*). The reaction was left at room temperature for 8 h, and the unincorporated pCp was removed via a Chroma spin 10 column (Clontech). Reaction products were purified on a 5% polyacrylamide, 8 M urea gel and isolated via the crush and soak method. Isolated products were ethanol-precipitated twice, dissolved in 200 μL of sterile water, and stored at −20 °C.

Determination of K_d for Binding to the Ribozyme. The ability of each 5′ exon mimic to bind the ribozyme was analyzed via competition with radiolabeled r(AUGACU) at 37 °C (*24*, *28*, *42*). The method used is essentially as described in the literature except that the ribozyme was reannealed at 55 °C for 10 min in 1X H15Mg buffer at pH 7.5. After an hour of incubation at 37 °C, the bound and the unbound oligonucleotides were separated on a 10% polyacrylamide gel containing H15Mg buffer and preequilibrated to 37 °C. The fraction r(AUGACU) bound (Θ) as a function of added competitor is given by (*43*, *44*)

$$\Theta = \frac{1}{2T_t}\left[K_t + \frac{K_t}{K_d}C_t + R_t + T_t - \sqrt{\left(K_t + \frac{K_t}{K_d}C_t + R_t + T_t\right)^2 - 4T_tR_t}\right] + A \quad (1)$$

where R_t, T_t, and C_t are the total concentrations of P-8/4x, radiolabeled r(AUGACU), and unlabeled competitor oligonucleotide, respectively; K_t is the dissociation constant for r(AUGACU) binding P-8/4x, determined from a direct gel binding assay (*24*); K_d is the dissociation constant for the competitor; and A is the fraction of r(AUGACU) apparently bound at infinite concentration of competitor. The latter corrects for a fraction of radioactivity that appears to bind covalently to the ribozyme. The competition curve is fit by nonlinear least squares for the best values of K_d, T_t, and A. All K_d values reported are the average of at least four independent measurements, and the errors given are the standard deviations in those repetitive measurements. The sequence d(ATGAmCm)rU bound too weakly to the ribozyme to afford accurate measurement of its K_d, so the value given is an estimate.

Optical Melting Experiments. All experiments were performed as described previously (*24*). In a typical experiment, an equal molar amount of r(GGUCAU) and diastereotopically pure methylphosphonate/DNA chimera or all-methylphosphonate oligonucleotide at a typical concentration range of 10−600 μM were mixed, dried in vacuo, and redissolved in the appropriate amount of H15Mg buffer. For melting curves, a temperature gradient from 0 to 60 °C was applied. The resulting absorbance versus temperature curves were fit to a two-state non-self-complementary model to extract thermodynamic parameters (*45*, *46*). The thermodynamic parameters were then obtained from both the average curve fit parameters and $1/T_M$ versus $\ln(C_T/4)$ plots. At least five different concentrations over a 60-fold range were analyzed for each sequence. Because of the low melting temperatures of these duplexes and the observation that r(GGUCAU) can form a self-complementary duplex, values for all thermodynamic parameters are considered to be estimates (*24*, *28*).

Trans-Splicing to Internally Labeled Precursor. All reactions were run in HXMg buffer at pH 6.5. The switch to pH 6.5 buffer was necessary to eliminate hydrolysis at the intron−3′ exon junction which occurs during the reaction and/or RNA reannealing periods. A solution containing internally labeled precursor in HXMg buffer was reannealed by heating at 55 °C for 5 min, cooled for 2 min at room temperature, and then incubated at 37 °C. Another solution containing 60 μM 5′ exon mimic and/or 2 mM pG in HXMg buffer and incubated at 37 °C for 5 min was added to an equal volume of the above precursor solution. A water control experiment was also performed. This reaction contained only precursor in HXMg buffer and was used to determine whether the presence of the 5′ exon−intron product is a result of the reaction conditions or is due to the presence of the 5′ exon mimic. Reactions were incubated at 37 °C for 1 h and stopped by the addition of a 2/3 volume of stop buffer. The 5′ exon−intron and intron splicing products were used to monitor trans- and cis-splicing, respectively. The 5′ exon−3′ exon and the 3′ exon products were not visible because of the low number of adenines in these products. Reaction products were separated on a 5% polyacrylamide, 8 M urea gel, and the radioactivity was quantified.

Splicing Kinetics. The rate of splicing, either trans or cis, was measured in H4Mg buffer at pH 6.5. In a typical reaction, the precursor solution was prepared as follows: 12 μL of internally labeled precursor was added to an equal volume of 2X H4Mg buffer and reannealed as described above. For the trans-splicing experiments, 24 μL of a solution containing 60 μM 5′ exon mimic in H4Mg buffer was added to the precursor solution at 37 °C. Cis-splicing experiments were initiated by adding 24 μL of a solution containing 2 mM pG in H4Mg buffer at 37 °C. These reactions were incubated at 37 °C, and 6 μL aliquots of the reaction mixture were removed at various times. Each aliquot was quenched by the addition of a 2/3 volume of stop buffer. Reaction products were separated on a 5% polyacrylamide, 8 M urea gel, and the radioactivity was quantified.

The observed rate constants for cis- and trans-splicing were measured by monitoring the amount of intron and 5′ exon−intron product, respectively, formed as a function of time. The fraction of trans- or cis-spliced products formed at time t, F_t, was divided by the fraction of maximum spliced product, F_∞, determined from the 60 min time point, and the observed rate constant for splicing, k_{obs}, determined from the least-squares fit to the following equation:

$$-k_{obs}t = \ln\left(1 - \frac{F_t}{F_\infty}\right) \quad (2)$$

The final values are given as the average of two experiments.

Dependence of Trans-Splicing on Oligonucleotide Concentration. A solution containing internally labeled precursor in H4Mg buffer at pH 6.5 was reannealed as described above and incubated at 37 °C. Then 3 μL of internally labeled precursor in H4Mg buffer was added to a 3 μL solution of serially diluted DNA or all-methylphosphonate 5′ exon mimic in H4Mg buffer. The solution was incubated at 37 °C for 1 h and then stopped by the addition of a 2/3 volume of stop buffer. Concentrations of 5′ exon mimic ranged from

Table 1: Calculation of BETI in H15Mg Buffer: Dissociation Constants for Binding to P-8/4X Ribozyme and to r((GGUCAU)[a]

	binding to the ribozyme		binding to r(GGUCAU)		tertiary interactions	
oligonucleotide	$K_{d,total}$ (nM)	$-\Delta G°_{37,total}$[b] (kcal/mol)	$K_{d,BP}$[b] (mM)	$-\Delta G°_{37,BP}$ (kcal/mol)	$-\Delta\Delta G°_{37,BETI}$[c] (kcal/mol)	K_2[d] "BETI"
d(AmTmGmAmCm)rU[e]	272 ± 79	9.31	8.32	2.95	6.36	30 600
d(ATGACm)rU (**1**)	202 ± 13	9.49	7.55	3.01	6.45	37 400
d(ATGACm)rU (**2**)	91 ± 42	9.99	4.13	3.38	6.61	45 500
d(ATGAmC)rU (**1**)[e]	99 ± 22	9.93	2.99	3.58	6.35	30 200
d(ATGAmC)rU (**2**)[e]	110 ± 30	9.87	2.42	3.58	6.29	22 000
d(ATGmAC)rU (**1**)	41 ± 30	10.50	15.40	2.57	7.93	376 000
d(ATGmAC)rU (**2**)	56 ± 19	10.30	13.50	2.65	7.65	242 000
d(AmTmGAC)rU (**1**)	157 ± 23	9.65	2.46	3.70	5.95	15 700
d(AmTmGAC)rU (**2**)	123 ± 15	9.80	2.76	3.63	6.17	22 400
d(AmTmGAC)rU (**3**)	94 ± 29	9.97	2.46	3.70	6.27	26 200
d(AmTmGAC)rU (**4**)	196 ± 7	9.51	2.27	3.75	5.76	11 600
d(ATGAmCm)rU (**1**)[f]	≈2 000		3.94	3.41		
d(ATGAmCm)rU (**2**)[f]	≈2 000		7.67	3.00		
d(ATGAmCm)rU (**3**)[f]	≈2 000		3.35	3.51		
d(AmTmGmAC)rU[e]	26 ± 22	10.80	7.31	3.03	7.77	281 000
d(ATGmAmCm)rU[e]	90 ± 65	9.99	4.87	3.28	6.71	54 100
d(ATGAC)rU[g]	61.1 ± 7	10.23	4.07	3.39	6.84	66 600
d(AnTnGnAnCn)rU[g]	16 ± 1	11.06	0.034	6.34	4.72	2 130
r(AUGACU)[h]	5.21 ± 1.4	11.75	0.32	4.96	6.79	61 000

[a] Ribozyme binding K_d values were determined via competitive gel binding assays in H15Mg buffer at pH 7.5. The thermodynamics for binding r(GGUCAU) were obtained from $1/T_M$ versus $\ln(C_T/4)$ plots. The letter m represents a methyl-phosphonate backbone. Numbers following the nucleotide sequence represent the methylphosphonate stereoisomers. The stereoisomers are numbered according to their relative elution on reverse-phase HPLC as described in the Materials and Methods section. The values reported are the average of at least four independent measurements, and the errors reported are the standard deviations in those repetitive measurements. [b] $\Delta G°_{37,total}$ is determined from the equation $\Delta G°_{37} = RT \ln(K_d)$ where $R = 0.001987$ kcal mol^{-1} K^{-1} and $T = 310$ K. [c] The free energy change of tertiary interactions is determined as the difference between the free energy of binding to the ribozyme and of binding to r(GGUCAU). [d] K_2 is a measure of the binding enhancement by tertiary interactions (BETI) and is determined by dividing the K_d for base pairing by the K_d for ribozyme binding. [e] The thermodynamics for forming these duplexes was determined from a racemic mixture. [f] This K_2, or BETI, was omitted because the binding to the ribozyme is too weak to reliably determine the $K_{d,total}$. [g] Reference *28*. Each n is a phosphoramidate linkage. [h] Reference *24*.

30 μM to 1.5 nM. Reaction products were separated on a 5% polyacrylamide, 8 M urea gel, and the radioactivity was quantified.

RESULTS

Methylphosphonate Stereoisomer Separation. For sequences containing one or two chiral methylphosphonate linkages (Figure 3), the stereoisomers were separated by HPLC (Figure 4). Both stereoisomers were separated and isolated for oligonucleotides containing one chiral center (d(ATGACm)rU, d(ATGAmC)rU, and d(ATGmAC)rU). The four stereoisomers of the sequence d(AmTmGAC)rU were also separated (Figure 4). The sequence d(ATGAmCm)rU, however, afforded complete isolation of only three species. The three species were present in an approximate ratio of 1:2:1 suggesting that *R,R* and *S,S* could be separated, but *R,S* and *S,R* could not.

Binding to the Ribozyme. The effect of methylphosphonate positional isomers and stereochemistry on binding to the ribozyme was determined for various 5′ exon mimics in H15Mg buffer at pH 7.5 (Figure 5, Table 1). All sequences with one methylphosphonate, d(ATGmAC)rU, d(ATGAmC)rU, and d(ATGACm)rU, bind to the ribozyme with similar K_d values of ≈100 nM (Table 1). The range in the K_d values of these three sequences is only about 5-fold. Thus, positional and stereochemical effects are small for single substitutions at the −1, −2, and −3 linkages of the oligonucleotide.

In contrast to the results for single substitutions, positional effects are large for doubly substituted sequences. The sequence d(AmTmGAC)rU binds with an average K_d of 143 nM, whereas d(ATGAmCm)rU binds with an average K_d of ≈2000 nM (Table 1). The latter K_d is at the experiment's upper limit and is considered an estimate. Thus, positional effects for the doubly substituted species could be even larger. The effect of stereochemistry on binding affinity of d(AmTmGAC)rU is only ≈2-fold (Table 1). Stereochemical effects also appear small for d(ATGAmCm)rU, but the gel binding assay could not precisely quantify the effect.

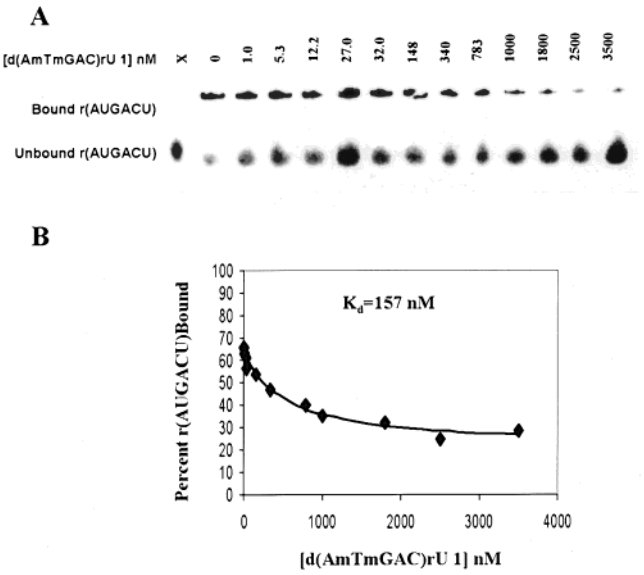

FIGURE 5: Typical competitive gel binding assay completed in H15Mg buffer at pH 7.5. The amount of unbound and bound radiolabeled r(AUGACU) is depicted as a function of added competitor, d(AmTmGAC)rU **1**, where the number after the oligonucleotide sequence refers to the relative elution of that stereoisomer on reverse-phase HPLC. (A) Autoradiogram of a typical gel completed in the presence of serially diluted d(AmTmGAC)rU **1**. (B) Typical titration curve and fit for this assay.

Table 2: Thermodynamics for Binding to r(GGUCAU) in H15Mg Buffer[a]

	thermodynamics obtained from $1/T_M$ vs $\ln(C_T/4)$ plots[b,c]				thermodynamics obtained from the average curve fits[b,c]			
oligonucleotide	$-\Delta G^\circ_{37}$ (kcal/mol)	$-\Delta H^\circ$ (kcal/mol)	$-\Delta S^\circ$ (eu)	T_M[d] (°C)	$-\Delta G^\circ_{37}$ (kcal/mol)	$-\Delta H^\circ$ (kcal/mol)	$-\Delta S^\circ$ (eu)	T_M[d] (°C)
d(AmTmGmAmCm)rU[e]	2.95 ± 0.10	63.56 ± 1.90	195.33 ± 6.48	20.4	3.31 ± 0.19	56.59 ± 3.21	171.79 ± 10.87	20.3
d(ATGACm)rU (**1**)	3.01 ± 0.36	53.49 ± 6.31	162.76 ± 21.36	17.8	3.26 ± 0.23	48.34 ± 3.27	145.37 ± 10.61	17.3
d(ATGACm)rU (**2**)	3.38 ± 0.38	47.96 ± 6.85	143.73 ± 23.18	17.9	3.30 ± 0.28	49.43 ± 2.37	148.72 ± 7.95	18.0
d(ATGAmC)rU[f]	3.58 ± 0.34	54.25 ± 7.94	163.36 ± 26.37	21.0	3.62 ± 0.31	51.66 ± 6.89	154.91 ± 22.74	20.5
d(ATGmAC)rU (**1**)	2.57 ± 0.09	72.05 ± 2.23	224.02 ± 7.42	20.9	3.27 ± 0.16	53.66 ± 4.83	162.46 ± 15.70	19.2
d(ATGmAC)rU (**2**)	2.65 ± 0.23	67.66 ± 5.26	209.62 ± 17.78	20.2	3.23 ± 0.26	53.78 ± 4.71	163.01 ± 15.71	19.0
d(AmTmGAC)rU (**1**)	3.70 ± 0.30	55.59 ± 7.86	167.29 ± 26.11	22.0	3.65 ± 0.12	57.34 ± 3.49	173.10 ± 11.37	22.2
d(AmTmGAC)rU (**2**)	3.63 ± 0.41	50.50 ± 8.24	151.10 ± 27.41	20.2	3.27 ± 1.27	52.48 ± 8.75	158.66 ± 74.10	18.8
d(AmTmGAC)rU (**3**)	3.70 ± 0.33	57.43 ± 6.42	152.44 ± 22.56	20.7	3.49 ± 0.16	57.43 ± 6.42	173.92 ± 20.73	21.4
d(AmTmGAC)rU (**4**)	3.75 ± 0.16	46.13 ± 3.83	136.65 ± 12.74	19.3	3.35 ± 0.27	56.55 ± 2.18	171.52 ± 7.34	20.5
d(ATGAmCm)rU (**1**)	3.41 ± 0.21	50.79 ± 4.45	152.76 ± 14.98	19.1	3.38 ± 0.33	51.66 ± 5.85	155.66 ± 19.87	19.2
d(ATGAmCm)rU (**2**)[f]	3.00 ± 0.31	56.36 ± 6.21	172.03 ± 21.00	18.7	3.35 ± 0.23	48.53 ± 4.60	148.67 ± 15.33	17.9
d(ATGAmCm)rU (**3**)	3.51 ± 0.01	52.39 ± 0.44	157.61 ± 1.49	20.1	3.36 ± 0.12	55.98 ± 1.25	169.50 ± 4.38	20.4
d(AmTmGmAC)rU[f]	3.03 ± 0.14	70.19 ± 4.00	216.54 ± 13.48	22.3	3.44 ± 0.12	57.01 ± 5.78	172.73 ± 18.78	21.1
d(ATGmAmCm)rU[f]	3.28 ± 0.35	58.67 ± 7.72	178.57 ± 25.91	20.7	3.41 ± 0.23	56.41 ± 4.96	170.88 ± 16.57	20.7
d(ATGAC)rU[g]	3.39 ± 0.16	56.73 ± 2.80	171.97 ± 9.40	20.7	3.51 ± 0.27	52.98 ± 6	159.49 ± 20	20.3
d(AnTnAnGnAnCn)rU[g]	6.34 ± 0.01	39.47 ± 0.50	106.80 ± 1.70	35.5	6.36 ± 0.21	46.77 ± 3.8	130.28 ± 12	35.9
r(AUGACU)[h]	4.96 ± 0.07	44.59 ± 1.80	127.76 ± 6.00	26.4	4.91 ± 0.07	46.41 ± 2.3	133.82 ± 7.6	26.5

[a] Oligonucleotides were melted in H15Mg buffer at pH 7.5. The letter m represents a methylphosphonate backbone. Numbers following the nucleotide sequence represent the methylphosphonate stereoisomers, which are numbered according to their relative elution on reverse-phase HPLC as described in the Materials and Methods section. [b] Due to the potential of r(GGUCAU) to self-associate, binding may be less favorable than indicated because the formation of $r(GGUCAU)_2$ may contribute to the thermodynamics. [c] Differences in the ΔH° of duplex formation greater than 15% may indicate non-two-state melting of these duplexes, and could be due to the stereotopic nature of some of the duplexes or to the low melting temperatures. [d] The T_M is calculated at 100 μM strand concentration. [e] The all-methylphosphonate oligonucleotide, d(AmTmGmAmCm)rU, is a mixture containing 32 stereoisomers. [f] The thermodynamics of d(ATGAmC)rU, d(AmTmGmAC)rU, d(ATGAmCm)rU (**2**), and d(ATGmAmCm)rU·r(GGUCAU) duplexes were determined for a methylphosphonate stereotopic mixture. [g] Reference *28*. Each n is a phosphoramidate linkage. [h] Reference *24*.

The triply substituted oligonucleotides, d(AmTmGmAC)rU and d(ATGmAmCm)rU, bind with an average K_d of 58 nM, and the difference in binding between the two positional isomers is ≈3-fold (Table 1). The all-methylphosphonate oligonucleotide, d(AmTmGmAmCm)rU, is a mixture of 32 stereoisomers and binds with a K_d of 272 nM (Table 1). As expected, a control sequence, d(CmAmGmTmAm)rU, did not bind to the ribozyme (Table 1).

Binding to r(GGUCAU) Hexamer. The thermodynamics of base-pairing to the hexamer, r(GGUCAU), to form a mimic of the ribozyme's P1 helix (Figure 1) were measured by thermal melting experiments in H15Mg buffer at pH 7.5 (Table 2). Single methylphosphonate linkages have a small effect on duplex stability when compared to unmodified d(ATGAC)rU. The strongest duplexes have a methylphosphonate linkage at and/or one nucleotide away from an end of the duplex (Table 2). The weakest duplexes have a substitution in the middle of the duplex, including the case when all linkages are methylphosphonates (Table 2). In all cases, stereochemistry does not affect the stability of the duplexes. In most instances, the differences in the thermodynamics of the duplexes are within experimental error.

Binding Enhancement by Tertiary Interactions (BETI). The binding enhancement by tertiary interactions (BETI) was quantified as the ratio of the K_d for base-pairing, determined from the $1/T_M$ versus ln ($C_T/4$) plots, to the K_d for binding to the ribozyme (Table 1). All sequences tested exploit BETI. The all-methylphosphonate oligonucleotide binds tightly to the ribozyme and exhibits a BETI of 30 600-fold (Table 1). These and previous results suggest the BETI is not a result of contacts with the 5′ exon mimic's 2′ hydroxyls (*24*) or the nonbridging oxygens of the 5′ exon mimic's backbone.

The result that tertiary contacts are not strongly dependent on the backbone of the 5′ exon mimic gives further evidence that the tertiary contacts may involve interactions between the intron and the IGS and not between the 5′ exon and the intron (*28*). The formation of the P1 helix may preorganize the IGS to participate in interactions that give rise to the BETI effect.

Effects of Oligonucleotides on Splicing of Internally Labeled Precursor as a Function of [Mg^{2+}]. Splicing assays were completed in HXMg buffer at pH 6.5. The pH 6.5 was chosen to eliminate hydrolysis at the intron−3′ exon junction that was observed at pH 7.5. The percentages of products derived from precursor splicing are depicted in Figure 6.

For one set of experiments, internally labeled precursor was incubated in a solution containing 30 μM of the 5′ exon mimic, d(ATGAC)rU, in HXMg buffer. In these experiments, the amount of intron formed from cis-splicing is negligible, because the guanosine cofactor necessary for cis-splicing is absent; the amount of 5′ exon−intron product formed is significant, however (Figure 6). At Mg^{2+} concentrations greater than 3 mM, the amount of trans-spliced product, 5′ exon−intron, rises to approximately 60% of the total radioactivity. This percentage remains constant until 9 mM Mg^{2+} and then decreases to 40% from 9 to 15 mM Mg^{2+}.

At a concentration of 30 μM, the all-methylphosphonate 5′ exon mimic, d(AmTmGmAmCm)rU, was also incubated with internally labeled precursor (Figure 6). The 5′ exon−intron product is also formed in this reaction and reaches a maximum at 4 mM Mg^{2+}, remains about 60% of the total radioactivity until 9 mM Mg^{2+}, and then decreases to approximately 30% from 9 to 15 mM Mg^{2+}. The 5′ exon−intron product formed with either d(ATGAC)rU or d(AmTmGmAmCm)rU could be created from two sources: oligonucleotide-induced hydrolysis or 5′ exon mimic reacting with precursor to form trans-spliced products.

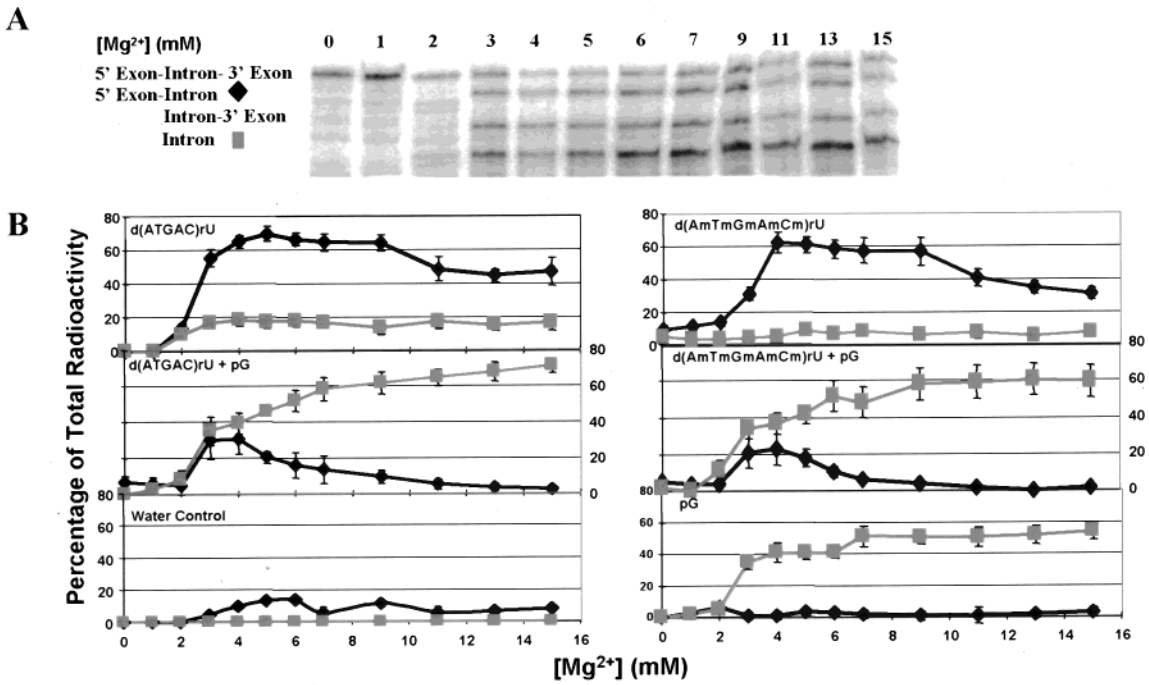

FIGURE 6: Trans-(◆) and cis-(■) splicing of internally labeled precursor measured in a variety of different conditions. All reactions were completed in HXMg buffer at pH 6.5. (A) Autoradiogram of a gel for a typical assay completed in 1 mM pG and 30 μM d(AmTmGmAmCm)rU. (B) Plots of data for various reaction conditions. Plots labeled d(ATGAC)rU and d(AmTmGmAmCm)rU correspond to splicing reactions completed with 30 μM of oligonucleotide. Plots labeled d(ATGAC)rU + pG and d(AmTmGmAmCm)rU + pG correspond to reactions in the presence of 1 mM pG and 30 μM oligonucleotide. Plots labeled pG correspond to reactions completed in the presence of 1 mM pG and the absence of oligonucleotide. The water control is a reaction completed in the absence of pG and oligonucleotide. This control shows that the 5′ exon−intron product is not formed during the reaction/reannealing conditions. All assays except for the water control are the average of four independent measurements. Error bars represent the standard errors for a given experimental point.

The ability of these 5′ exon mimics to inhibit normal splicing in the presence of 1 mM pG was analyzed at a 5′ exon mimic concentration of 30 μM (Figure 6). In both the DNA and the all-methylphosphonate cases, the amount of 5′ exon−intron product formed is approximately equal, within experimental error, to the amount of normally spliced intron formed when the Mg^{2+} concentration is 3−4 mM. At concentrations greater than 5 mM Mg^{2+} almost no 5′ exon−intron product is observed. At all Mg^{2+} concentrations, the amount of fully spliced intron is approximately equal to that in the cis-spliced pG reaction completed in the absence of oligonucleotide. Thus, there is no evidence for inhibition of cis-splicing, even though the hexamers induce formation of 5′ exon−intron product. The results suggest that d(ATGAC)-rU and d(AmTmGmAmCm)rU cannot compete with intramolecular base-pairing when the precursor is folded correctly for cis-splicing.

A water control was performed to ensure that formation of the 5′ exon−intron product was induced by the 5′ exon mimics or the guanosine cofactor (Figure 6). This experiment shows that only an insignificant amount of 5′ exon−intron and intron products are formed without the addition of oligonucleotide or pG, as expected.

Effects of Oligonucleotides on Splicing with 3′ End-Labeled Precursor as a Function of [Mg^{2+}]. Splicing assays using 3′ end-labeled precursor were completed in HXMg buffer at pH 6.5 (Figure 7). This allowed determination of the source of the 5′ exon−intron product observed in assays using internally labeled precursor, since 3′ end-labeled material allows visualization of both the trans-spliced and the hydrolysis products. Reactions were started by adding

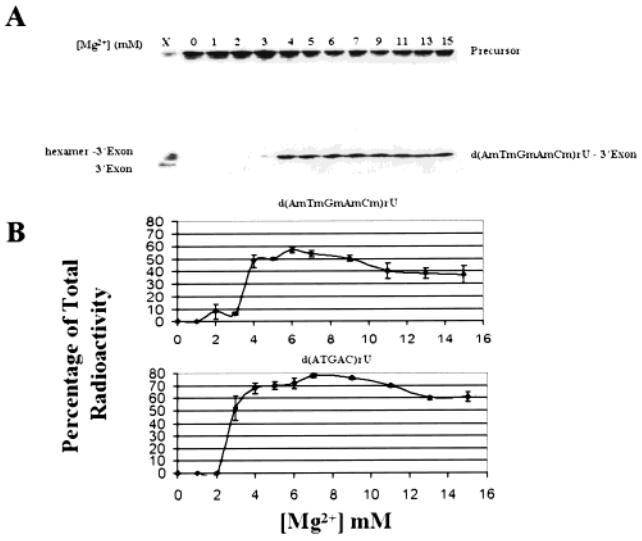

FIGURE 7: Splicing measured with 3′ end-labeled precursor in 30 μM d(AmTmGmAmCm)rU and HXMg buffer at pH 6.5. (A) Autoradiogram of a gel for a typical assay completed with 30 μM d(AmTmGmAmCm)rU. Lane X presents markers for hydrolysis and trans-spliced, hexamer−3′exon products. (B) Plots of data obtained for reactions. Each plot is the average of two independent experiments, and the errors given are the standard errors.

30 μM of either d(ATGAC)rU or d(AmTmGmAmCm)rU to 3′ labeled precursor. The formation of 3′ exon, a result of oligonucleotide-induced hydrolysis, and the 5′ exon mimic−3′ exon, a result of trans-splicing, was measured as a function of Mg^{2+} concentration.

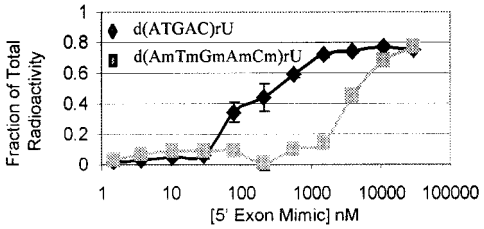

FIGURE 8: Oligonucleotide concentration dependence of trans-splicing in the absence of pG measured in H4Mg buffer at pH 6.5. The plot represents data from 1 h reactions with either d(AmTmGmAmCm)rU (■) or d(ATGAC)rU (◆). Each plot is the average of two independent measurements, and the errors given are the standard errors.

Table 3: Summary of the Rates and Half-Lives for Normal (Cis-) and Trans-Splicing

	d(ATGAC)rU[a]	d(AmTmGmAmCm)rU[a]	pG[b]
k (min^{-1})	0.077	0.057	0.113
$t_{1/2}$ (min)	9.0	12.1	6.2

[a] Trans-splicing rates and half-lives were measured by monitoring the formation of the 5′exon−intron product in the presence of 30 μM d(ATGAC)rU or d(AmTmGmAmCm)rU using internally labeled precursor. [b] Normal cis-splicing rates were measured by monitoring the formation of the intron product in the presence of 1 mM pG. All assays were completed at 37 °C, pH 6.5, and 4 mM Mg^{2+}. Errors are typically ±10%. All values are the average of two independent measurements.

When these reactions were completed in the presence of either the DNA or the all-methylphosphonate 5′ exon mimics at concentrations of 30 μM, trans-spliced products were seen exclusively (Figure 7). Furthermore, the efficiency and the Mg^{2+} dependence of splicing with internally labeled and 3′ end-labeled precursor are essentially the same, indicating that both assays monitor the same reaction. Thus, the 5′ exon−intron product in the internally labeled precursor experiments is a result of trans-splicing (Figures 6 and 7).

The sequence dependence of trans-splicing with 3′ end-labeled precursor was also tested in HXMg buffer (data not shown). The control reverse sequences, d(CAGTA)rU and d(CmAmGmTmAm)rU, were added at a concentration of 30 μM. No trans-spliced or hydrolysis products were observed: trans-splicing is sequence specific as expected.

Dependence of Trans-Splicing on Oligonucleotide Concentration. The amount of trans-spliced product formed as a function of 5′ exon mimic concentration was analyzed with internally labeled precursor in H4Mg buffer at pH 6.5 (Figure 8). For d(AmTmGmAmCm)rU and d(ATGAC)rU, the amount of 5′ exon−intron product, indicative of trans-splicing, exceeded about 50% of the total radioactivity from 4 to 30 μM and 0.25−30 μM of oligonucleotide, respectively. This 16-fold difference could be partially due to the decreased binding of d(AmTmGmAmCm)rU when compared to d(ATGAC)rU (Table 1).

Kinetics of Cis- and Trans-Splicing. The kinetics of cis- and trans-splicing were measured with internally labeled precursor in H4Mg buffer at pH 6.5 (Table 3, Figure 9). The observed rate constant of trans-splicing was measured in the presence of 30 μM DNA or all-methylphosphonate 5′ exon mimic. Both d(ATGAC)rU and d(AmTmGmAmCm)-rU trans-splice with similar observed rate constants. Cis-splicing was measured with precursor incubated in 1 mM pG (Table 3). The observed rate constants of both trans- and cis-splicing reported here at pH 6.5 are similar to those previously determined for *P. carinii* and the *Tetrahymena thermophila* precursors at pH 7.5 (*24*, *47*); thus, changing the pH from 7.5 to 6.5 has little effect on the splicing reactions.

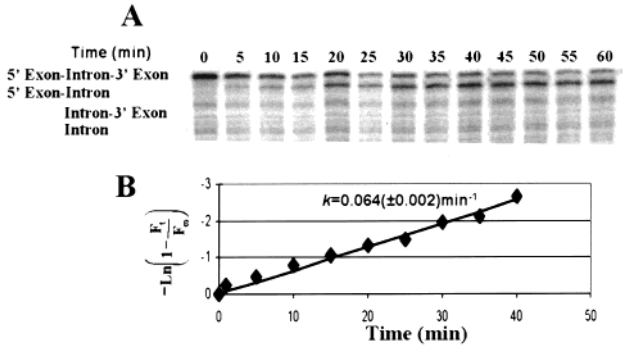

FIGURE 9: Rate of splicing measured with 30 μM d(ATGAC)rU or d(AmTmGmAmCm)rU in H4Mg buffer at pH 6.5. (A) Autoradiogram of a gel for a typical assay completed with 30 μM of d(AmTmGmAmCm)rU. (B) The above data fit to a pseudo-first-order rate plot. The observed rate constant, $k_{obs} = 0.064 \pm 0.002$ min^{-1}, is determined as the slope of the pseudo-first-order rate plot. Error is calculated from the error in the linear regression.

DISCUSSION

The results presented here show that an uncharged methylphosphonate oligonucleotide, with a sequence that mimics the 3′ end of the natural 5′ exon, binds to the group I ribozyme (Table 1) and reacts with a truncated ribosomal RNA precursor from mouse-derived *P. carinii* (Figures 6 and 7). This expands the range of small oligonucleotides that may be used to target the tertiary folding of large RNAs through binding enhanced by tertiary interactions and suicide inhibition strategies (*24*, *28*, *29*). Such antisense agents can have unexpected target affinity and specificity compared to their larger counterparts (Table 1) (*24*), because they recognize the RNA based on the global architecture of 100 or more nucleotides. Oligonucleotides designed with these principles should be less expensive, have fewer side-effects, and perhaps cross cellular membranes more effectively than larger oligonucleotides (*4*, *5*).

Base-Pairing of Methylphosphonate Oligonucleotides to r(GGUCAU). Previous experiments have shown that the duplex stabilities of helices containing methylphosphonate linkages are highly stereospecific (*48*, *49*). A study of the T_M values of dT methylphosphonate octanucleotides pairing to dA pentanucleotide revealed that duplexes where six of the strand's linkages are composed of the R stereoisomer had a T_M that was at least 30 °C higher than that of a similar duplex where six of the linkages are composed of the *S* stereoisomer, and 20 °C higher than that of the corresponding DNA duplex (*49*). Optical melting experiments on non-self-complementary duplexes, in which one of the strands contained either the *R* or the *S* stereoisomers and the other strand was DNA, show melting behaviors that are sequence specific (*50*). The data in Table 2 suggest that methylphosphonate substitutions have an insignificant effect on the melting of the r(GGUCAU)/d(ATGAC)rU duplex. The smaller effects observed with this duplex may be due to the fact that it is an RNA/DNA hybrid, or that it is shorter than duplexes measured in previous studies, or may be due to other factors.

Tertiary Interactions. Potential tertiary interactions involving nonbridging oxygens were probed by replacing the negatively charged phosphodiester groups with neutral methylphosphonates (Figure 3). Binding to ribozyme is insignificantly changed when a single methylphosphonate group is substituted for a phosphodiester in d(ATGmAC)rU, d(ATGAmC)rU, and d(ATGACm)rU (Table 1). The sequences d(AmTmGAC)rU, d(AmTmGmAC)rU, d(ATGmAmCm)rU, and d(AmTmGmAmCm)rU also bind as well as the DNA substrate (Table 1). The binding of d(ATGAmCm)rU, however, is weaker ($K_d \approx 2000$ nM). The weak binding of d(ATGAmCm)rU cannot be due to base-pairing considerations because, as indicated by the optical melting experiments, this sequence can base-pair as well as the other hexamers with the IGS (Table 2). Evidently, d(ATGAmCm)rU has altered tertiary contacts. Previous studies have shown that substituting methylphosphonates for phosphodiesters can induce bending in oligonucleotides (*51*). Perhaps the two substitutions in d(ATGAmCm)rU induce such a structural change and cause the reduced binding of this oligonucleotide. Analysis of the binding data indicates that adding a methylphosphonate linkage between G-4 and A-3, to give d(ATGmAmCm)rU, "rescues" binding of d(ATGAmCm)rU (Table 1). Interestingly, the singly substituted d(ATGmAC)rU has the weakest equilibrium constant for base-pairing but the largest BETI (Tables 1 and 2). There are several possible explanations, including the following: (1) the substitution in the middle of the duplex may preorganize the oligonucleotide for binding to the ribozyme; and (2) there may be unfavorable tertiary interactions with the phosphate group between G-4 and A-3, and these are relieved by the methylphosphonate substitution.

Because they are stereotopic, methylphosphonates provide information on stereochemical as well as positional effects of replacing a nonbridging oxygen with a methyl group. Analysis of the binding data shows that the stereochemistry of the uncharged methylphosphonate group has little or no effect on the ability of the intron to recognize 5′ exon mimics.

The strong binding of the all-methylphosphonate oligonucleotide and the previously reported DNA oligonucleotide (*24*) suggests that both the phosphodiester backbone and the 2′ hydroxyls of the 5′ exon mimic are not directly involved in forming favorable tertiary contacts with the intron's catalytic core. This is surprising considering the large number of tertiary contacts in the active sites of catalytic RNAs such as the *T. thermophila* group I intron and group II introns (*9, 15*−*19, 52*−*56*). Perhaps the tertiary interactions reside on the IGS strand of the P1 helix and not on the 5′ exon mimic (*28*). Alternatively, lost favorable tertiary interactions may be compensated for by formation of new favorable interactions or removal of unfavorable interactions.

Comparison of the Ability of Methylphosphonate and DNA Substrates to Splice to the 3′ Exon. At concentrations of 30 μM, both the DNA and the all-methylphosphonate substrates exhibit similar trans-splicing profiles regardless of whether the reaction is competing with cis-splicing in the presence of pG (Figures 6 and 7). There are only slight differences in the observed rate constants of trans-splicing of the deoxyhexamers with phosphodiester, 0.077 min^{-1}, or all-methylphosphonate backbones, 0.057 min^{-1} (Table 3). The splicing kinetics at 30 μM suggest that the reactivities of the bound all-methylphosphonate and the DNA substrates are similar. The dependence of splicing efficiency on oligonucleotide concentration, however, suggests a difference in their binding to the precursor. The DNA substrate forms trans-spliced products at an efficiency of 50% at concentrations as low as 250 nM; the all-methylphosphonate substrate, however, requires concentrations of at least 4 μM to splice with 50% efficiency (Figure 8).

Comparison of splicing in the presence of pG and of the all-methylphosphonate or the DNA 5′ exon mimics with the previously reported results for phosphoramidate hexanucleotide (*29*) shows that all-methylphosphonate and DNA mimics are less effective cis-splicing inhibitors than the phosphoramidate hexanucleotide. These differences could be due to the differential binding of these oligonucleotides (Table 1) or structural differences. NMR structures of phosphoramidate duplexes show that these oligonucleotides are more similar in structure to RNA than to DNA (*57, 58*). If oligonucleotide trans-splicing in the presence of pG is sensitive to structural perturbations, oligonucleotides that look more like RNA may be better suicide inhibitors.

Development of Therapeutics Targeting P. carinii's Group I Intron. The observation that all-methylphosphonate and DNA 5′ exon mimics can react with the *P. carinii* large subunit rRNA precursor to form trans-spliced products makes the all-methylphosphonate, the DNA, and various chimeric 5′ exon mimics potential drug candidates. Since in vitro self-splicing conditions do not exactly mimic those in vivo (*59*), the 5′ exon mimics could be more or less potent inhibitors of self-splicing in animals or cell culture.

All pharmaceuticals that target an organism must permeate cellular membranes to be effective. The oligonucleotides studied here have potential advantages with regard to cellular uptake. Most importantly, smaller oligonucleotides are known to be taken up by cells in much higher concentrations than their larger counterparts (*4, 5*). In addition, methylphosphonate oligonucleotides are known to be taken up by cells by either passive diffusion (*5, 60*) or non-receptor-mediated endocytosis (*61*). Because little is known about fungal cell walls and whether fungi shuttle nucleic acids, oligonucleotides that passively diffuse through cells may be advantageous for achieving high intracellular concentrations. The results presented here show that the BETI approach can be implemented with small oligonucleotides having no charge or reduced charge due to methylphosphonate substitutions. Thus charge can be varied to improve cellular uptake and other important pharmacological properties.

ACKNOWLEDGMENT

The authors thank Jess Childs and Karina Burkard for critical reading of the manuscript and Mark Burkard for helpful discussions. M.D.D. also thanks Professor Jeff Davis (University of Maryland, College Park, MD) for chemical inspiration.

REFERENCES

1. Uhlman, E., and Peyman, A. (1990) *Chem. Rev. 90*, 543−584.
2. Herschlag, D. (1991) *Proc. Natl. Acad. Sci. U.S.A. 88*, 6921−6925.
3. Wagner, R. W., Matteucci, M. D., Grant, D., Huang, T., and Froehler B. C. (1996) *Nat. Biotechnol. 14*, 840−844.

4. Loke, S. L., Stein, C. A., Zhang, X. H., Mori, K., Nakanishi, M., Subbainghe, C., Cohen, J. S., and Neckers, L. M. (1989) *Proc. Natl. Acad. Sci. U.S.A. 86*, 3474−3478.
5. Jaroszewski, J. W., and Cohen, J. S. (1991) *Adv. Drug Delivery Rev. 6*, 235−250.
6. Cech, T. R., and Golden, B. L. (1999) in *The RNA World: The Nature of Modern RNA Suggests a Prebiotic RNA* (Gesteland, R. F., Cech, T. R., and Atkins, J. F., Eds.) 2nd ed., pp 321−349, Cold Spring Harbor Laboratory Press, Cold Spring Harbor, NY.
7. Cech, T. R. (1990) *Annu. Rev. Biochem. 59*, 543−568.
8. Cech, T. R., Herschlag, D., Piccirilli, J. A., and Pyle, A. M. (1992) *J. Biol. Chem. 267*, 17479−17482.
9. Bevilacqua, P. C., and Turner, D. H. (1991) *Biochemistry 30*, 10632−10640.
10. Bevilacqua, P. C., Kierzek, R., Johnson, K. A., and Turner, D. H. (1992) *Science 258*, 1355−1358.
11. Banerjee, A. R., Jaeger, J. J., and Turner D. H. (1993) *Biochemistry 32*, 153−163.
12. Bevilacqua, P. C., Sugimoto, N., and Turner, D. H. (1996) *Biochemistry 35*, 648−658.
13. Herschlag, D., and Cech, T. R. (1990) *Biochemistry 29*, 10159−10171.
14. Herschlag, D. (1992) *Biochemistry 31*, 1386−1399.
15. Piccirilli, J. A., Vyle, J. S., Caruthers, M. H., and Cech, T. R. (1993) *Nature 361*, 85−88.
16. Pyle, A. M., and Cech, T. R. (1991) *Nature 350*, 628−631.
17. Pyle, A. M., Murphy, F. L., and Cech, T. R. (1992) *Nature 358*, 123−128.
18. Strobel, S. A., and Cech, T. R. (1993) *Biochemistry 32*, 13593−13604.
19. Sugimoto, N., Tomka, M., Kierzek, R., Bevilacqua, P. C., and Turner, D. H. (1989) *Nucleic Acids Res. 17*, 355−371.
20. Liu, Y., and Leibowitz, M. J. (1995) *Nucleic Acids Res. 23*, 1284−1290.
21. Mei, H.-Y., Cui, M., Lemrow, S. M., and Czarnik, A. W. (1997) *Bioorg. Med. Chem. 5*, 1185−1195.
22. Nikolcheva, T., and Woodson, S. A. (1997) *RNA 3*, 1016−1027.
23. Liu, Y., Rocourt, M., Pan, S., Liu, C., and Lebowitz, M. J. (1992) *Nucleic Acids Res. 20*, 3763−3772.
24. Testa, S. M., Haidaris, C. G., Gigliotti, F., and Turner, D. H. (1997) *Biochemistry 36*, 15303−15314.
25. Gonzales-Martin, G., Yanez, C. G., Gonzalez-Contreras, L., and Labarca, J. (1999) *Int. J. Clin. Pharm. Ther. 37*, 34−40.
26. Gordin, F. M., Simon, G. L., Wofsy, C. B., and Mills, J. (1984) *Ann. Inter. Med. 100*, 495−499.
27. Sternberg, S. (1994) *Science 266*, 1632−1634.
28. Testa, S. M., Gryaznov, S. M., and Turner D. H. (1998) *Biochemistry 37*, 9379−9385.
29. Testa, S. M., Gryaznov, S. M., and Turner, D. H. (1999) *Proc. Natl. Acad. Sci. U.S.A. 96*, 2734−2739.
30. Miller, P. S. (1991) *Bio/Technology 9*, 358−362.
31. Pennisi, E. (1998) *Science 279*, 1129−1131.
32. Good, N. E., Winget, G. D., Winter, W., Connolley, T. N., Izawa, S., and Singh, R. M. M. (1966) *Biochemistry 5*, 467−477.
33. Ogilvie, K. K., Usman, N., Nicoghosian, K., and Cedergren, R. J. (1988) *Proc. Natl. Acad. Sci. U.S.A. 85*, 5764−5768.
34. Usman, N., Ogilvie, K. K., Jiang, M.-Y., and Cedergren, R. J. (1987) *J. Am. Chem. Soc. 109*, 7845−7854.
35. Stawinski, J., Stromberg, R., Thelin, M., and Westman, E. (1988) *Nucleic Acids Res. 16*, 9285−9298.
36. Wincott, F., DiRenzo, A., Shaffer, S., Grimm, S., Tracz, D., Workman, C., Sweedler, D., Gonzalez, C., Scaringe, S., and Usman, N. (1995) *Nucleic Acids Res. 23*, 2677−2684.
37. Miller, P. S., Yano, J., Carroll, C., Jayaraman, K., and Ts'o, P. O. P. (1979) *Biochemistry 23*, 5134−5143.
38. Miller, P. S., Agris, C. H., Blandin, M., Murikami, A., Reddy, P. M., Spitz, S. A., and Ts'o, P. O. P. (1983) *Nucleic Acids Res. 11*, 5189−5204.
39. Miller, P. S., Reddy, M. P., Murakami, A., Blake, K. R., Lin, S., and Agris, C. H. (1986) *Biochemistry 25*, 5092−5097.
40. Hogrefe, R., Vaghefi, M. M., Reynolds, M. A., Young, K. M., and Arnold, L. J. (1993) *Nucleic Acids Res. 21*, 2031−2038.
41. Romaniuk, P. J., and Uhlenbeck, O. C. (1983) *Methods Enzymol. 100*, 52−59.
42. Strobel, S. A., and Cech, T. R. (1993) *Biochemistry 32*, 13593−13604.
43. Lin, S., and Riggs, A. R. (1972) *J. Mol. Biol. 72*, 671−690.
44. Weeks, K. M., and Crothers, D. M. (1992) *Biochemistry 31*, 10281−10287.
45. McDowell, J. A., and Turner D. H. (1996) *Biochemistry 35*, 14077−14089.
46. Longfellow, C. E., Kierzek, R., and Turner D. H. (1990) *Biochemistry 29*, 278−285.
47. Bass, B., and Cech, T. R. (1984) *Nature 308*, 820−826.
48. Bower, M., Summers, M. F., Powell, C., Shinozuke, K., Regan, J., Zon, G., and Wilson, W. D. (1987) *Nucleic Acids Res. 15*, 4915−4930.
49. Lesnikowshi, Z. J., Jaworska, M., and Stec, W. J. (1990) *Nucleic Acids Res. 18*, 2109−2115.
50. Kibler-Herzog, L., Zon, G., Uzanski, B., Whittier, G., and Wilson, W. D. (1991) *Nucleic Acids Res. 19*, 2979−2986.
51. Strauss, J. K., and Maher, L. J. (1994) *Science 266*, 1829−1834.
52. Michel, F., and Westof, E. (1990) *J. Mol. Biol. 216*, 585−610.
53. Pyle, A. M., Moran, S., Strobel, S. A., Chapman, T., Turner, D. H., and Cech, T. R. (1994) *Biochemistry 33*, 13856−13863.
54. Strobel, S. A., and Ortoleva-Donnelly, L. (1999) *Chem. Biol. 6*, 153−165.
55. Szewczak, A. A., Ortoleva-Donnelly, L., Zivarts, M. V., Oyelere, A. K., Kazanisev, A. V., and Strobel, S. A. (1999) *Proc. Natl. Acad. Sci. U.S.A. 96*, 11183−11188.
56. Abramovitz, D. L., Friedman, R. A., and Pyle, A. M. (1996) *Science 271*, 1410−1413.
57. Ding, D., Gryaznov, S. M., Lloyd, D. H., Chandrasekaran, S., Yao, S., Ratmeyer, L., Pan, Y., and Wilson, W. D. (1996) *Nucleic Acids Res. 24*, 354−360.
58. Ding, D., Gryaznov, S. M., and Wilson, W. D. (1998) *Biochemistry 37*, 40160−4167.
59. Nikolcheva, T. and Woodson, S. A. (1999) *J. Mol. Biol. 292*, 557−567.
60. Shoji, K., Akhtar, S., Periasamy, A., Herman, B., and Juliano, R. L. (1991) *Nucleic Acids Res. 19*, 5543−5550.
61. Levis, J. T., Butler, W. O., Tseng, B. Y., and Ts'o, P. O. P. (1995) *Antisense Res. Dev. 5*, 251−259.

BI992937M